

## Experimental electron energy-loss spectra and cross sections for the $5^2S \rightarrow 5^2P^o$ transition in Cd II

Ara Chutjian

*Jet Propulsion Laboratory, California Institute of Technology, Pasadena, California 91109*

(Received 11 July 1983)

Experimental energy-loss spectra for excitation of the  $5^2S \rightarrow 5^2P^o$  transition in Cd II by electrons have been observed for the first time. Differential scattering cross sections are reported from spectra obtained at 75-eV electron energy. Comparisons are made to experimental results for the  $^2S_{1/2} \rightarrow ^2P_{3/2}$  integral excitation cross section from absolute emission measurements on the 214.4-nm ( $^2P_{3/2} \rightarrow ^2S_{1/2}$ ) transition, to theoretical results for the analogous  $4^2S \rightarrow 4^2P^o$  transition in Zn II, and to semiempirical calculations in the Gaunt-factor approximation. A detailed description of the crossed (90°) electron-beam-ion-beam apparatus is given, and the method of conversion of scattering intensity to absolute cross section is discussed.

### I. INTRODUCTION

Within this last decade increasing emphasis has been placed on understanding high electron-temperature plasmas. Such plasmas are encountered in astronomy during observations of stellar objects, the interstellar medium, and the Io-Jupiter torus by earth-orbiting satellites such as SKYLAB<sup>1</sup> and the International Ultraviolet Explorer (IUE),<sup>2</sup> and by the Voyager-1 and Voyager-2 spacecrafts.<sup>3</sup> Somewhat closer to home, the development of fusion reactors such as the Joint European Torus<sup>4</sup> (JET) and the Princeton Tokamak Fusion Test Reactor<sup>5</sup> (TFTR) involves the characterization and modeling of the rich emissions observed in these discharges.<sup>6</sup>

An important part of the data base needed for modeling these plasmas are electron-ion collision cross sections for ionization and excitation of the target ion, as well as for dielectronic recombination. However, because of the low ion target densities available in laboratory measurements (less than  $10^8 \text{ cm}^{-3}$ ), such studies of cross sections and phenomena are made tedious and difficult. Nevertheless, several recent and interesting developments have increased our understanding of electron-ion collision phenomena. Observations of inelastic electron scattering in Zn II by Chutjian and Newell<sup>7</sup> and Chutjian *et al.*<sup>8</sup> in a crossed-beam (90°) experiment, of dielectronic recombination in Mg II by Belić *et al.*<sup>9</sup> (crossed-beam geometry) in C II by Mitchell *et al.*,<sup>10</sup> and in B III and C IV by Dittner *et al.*<sup>11</sup> (merged-beam geometries) have provided exciting new approaches to our understanding of high-temperature plasmas. Cross-section measurements for these newly observed phenomena will complement the body of measurements already extensively reported in the literature for electron-ion excitation and ionization processes.<sup>12</sup>

In this paper we present the first reported measurements for inelastic electron scattering from Cd II.<sup>13</sup> In particular, we report energy-loss<sup>7</sup> spectra for the  $5^2S \rightarrow 5^2P^o$  transition at 75-eV incident electron energy, and the angular distribution of this inelastic feature at the same energy, over the angular range  $4^\circ \leq \theta \leq 16^\circ$ . The

$e$ -Cd II system is interesting because the excitation involves the next higher resonance transition to Zn II, for which experimental<sup>7,8,14</sup> and theoretical<sup>15</sup> data have been reported. Thus the measurement of trends between  $n=4$  (Zn II) and  $n=5$  (Cd II) can offer insight into the important effects which influence the magnitude and shape of inelastic cross sections. Once theoretical codes can confidently be used to account for these trends they can, for example, be used to calculate cross sections in multiply charged ions which are significant components of astronomical and fusion plasmas, and for which measurements are even more difficult.

The upper states  $5p^2P$  and  $4d^95s^2D$  in Cd II have received attention for their role in the He-Cd II hollow-cathode laser.<sup>16-18</sup> One finds the surprising result that these states appear to be excited preferentially by electrons rather than by the usual Penning ionization process. Also, one finds electron impact cross sections for the so-called Beutler  $^2D$  state (arising from the excited inner-shell configuration  $\dots 4d^95s^2$ ) to be comparable to, or to exceed that for the  $^2P$  resonance state.<sup>18</sup> One would thus expect cross-section measurements in singly charged metal ions to have bearing in modeling the performance of many hollow-cathode laser systems, and to offer some surprises as well.

In Sec. II we present details of the experimental apparatus and techniques used in obtaining both the present  $e$ -Cd II results, as well as those in the  $e$ -Zn II system.<sup>7,8</sup> Differential and integral cross sections are discussed in Sec. III where comparison is made with line-emission measurements of Hane *et al.*,<sup>18</sup> and with semiempirical (Gaunt-factor) calculations from results of Mewe.<sup>19</sup>

### II. EXPERIMENTAL CONSIDERATIONS

The apparatus used in these measurements utilized a 90° crossed electron-ion beam geometry. A schematic diagram of the apparatus is shown in Fig. 1. Singly ionized cadmium ions were generated in a discharge ion source<sup>20</sup> using metallic cadmium, without use of a carrier gas.

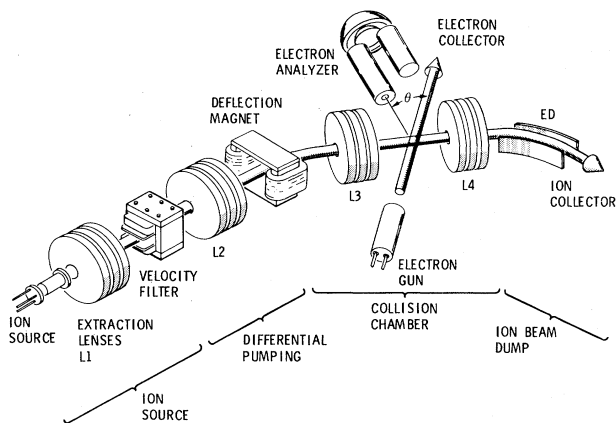


FIG. 1. Schematic diagram of the crossed electron-ion beam apparatus. Three-element lenses are indicated by L1, L2, L3, and L4, and electrostatic deflector by ED. The electron scattering angle  $\theta$  is shown. Length of apparatus from ion source to ion collector is 230 cm.

Ions were extracted through a 0.5-mm-diam anode hole by a series of lenses L1 (Fig. 1) and velocity analyzed in a Wien filter. The ion-source region was pumped by a single oil-diffusion pump having a manufacturer-stated pumping speed of 250 l/s at the source. Typical pressure in this region was  $\sim 5 \times 10^{-5}$  Pa ( $4 \times 10^{-7}$  Torr) during operation of the source, with a base pressure of  $4 \times 10^{-6}$  Pa.

Velocity selected ions after the Wien filter were focused by a three-element cylinder lens L2 used as an einzel lens. This section of the ion-beam line was differentially pumped by two oil-diffusion pumps providing 100-l/s speed at the beam area, and having a narrow connecting channel of conductivity 8 l/s. Ions after L2 were deflected by a box-type magnet, and focused by a three-element lens L3 to a calculated spot size of about 1.8-mm diam at the collision center. After the focus the ions were intercepted by the three-element lens L4, electrostatically deflected (ED) through an angle of  $60^\circ$  and focused into a deep Faraday cup. Currents of 2–5  $\mu\text{A}$  at 6-keV beam energy were measured at this point. Also, the Faraday cup and collision chamber were separately pumped by a 250-l/s oil-diffusion pump. Typical pressure in the collision region with both ion and electron beams running was  $2 \times 10^{-6}$  Pa, with a base pressure of  $6 \times 10^{-7}$  Pa.

A beam of electrons was focused onto the ion beam and scattered electrons were detected by a rotatable, hemispherical electrostatic analyzer. Early in the design of the apparatus it was decided that, despite the expected low levels of signal ( $\sim 10^2$  Hz) relative to an expected high background level, electron-beam collimation would be favored over high beam current with its concomitant larger spatial beam spread. This would permit measurements at lower scattering angles (close to  $0^\circ$ ) and better trapping of the incident beam, thus minimizing parent beam-signal interference. Towards this end an electron gun was designed which allowed control over the final beam angle by means of an einzel (field) lens, and control over the final beam focus by means of a variable-focus (zoom) lens as well. The design arrived at consisted of an

electron-gun system described earlier<sup>21</sup> with an added field lens. A total of seven lenses was used. Calculated final beam plus pencil half angles at the scattering center were  $0.2^\circ$ – $0.1^\circ$  and calculated beam diameters 2.3–1.3 mm, in the electron energy range  $E_0 = 7.5$ –150 eV. Measured beam currents were 0.5–4  $\mu\text{A}$  in this same energy range. It thus appears that, from considerations of space-charge limited currents, the calculated small beam divergence was not realized in practice, but divergences were more likely in the range  $1.5^\circ$ – $0.5^\circ$ . The energy spread in the incident beam, as measured from inelastic scattering features in Ar and Cd II, was 0.55 eV [full width at half maximum (FWHM)]. A more complete description of this gun will be published later.

The hemispherical analyzer and associated lens system were described earlier.<sup>21</sup> The hemispheres had a mean radius of 1.8 cm and a resolution of 0.14 eV (FWHM) at the center energy (4 eV) used in the measurements. The maximum acceptance half angle of the analyzer lens system was  $2^\circ$  as determined by the geometry of the entrance apertures. The analyzer system was mounted on a rotatable gear wheel whose plane was normal to the direction of the incident ion beam. A hole cut in the center of the gear allowed passage of the ion beam.

Care was taken to shield electrically the gun and analyzer lens elements near the scattering center, as well as all high- and low-voltage hookup wires. Materials in the vicinity of the scattering center were nonmagnetic metals such as beryllium-copper (gear), molybdenum (ion-beam aperture), copper (electron Faraday cup), and degaussed 304 stainless steel (auxiliary atomic beam source). Electron lens elements and hemispheres were machined from molybdenum. The collision chamber was lined with one layer of 1.5-mm-thick magnetic shielding which reduced the residual magnetic field at the collision area (including the analyzer system) to less than  $10^{-6}$  T. The presence of stray fields was checked by (a) measuring the shape of a known angular differential cross section in argon and (b) detecting any change in the incident electron beam current as voltages to the electron analyzer and detector were increased to their operational values.

Typical focusing procedures used in both the Zn II and Cd II measurements were to first focus the electron gun and analyzer on the argon 11.828 eV [ $^1S_0 \rightarrow 4s'(1/2)'(1P_1)$ ] resonance transition at the desired incident electron energy (here, 75 eV). This focus was determined by maximizing the electron current into its collector, and maximizing the inelastic signal as well. The argon beam was pumped away and the ion beam turned on. (At times, the focusing was done in the presence of the ion beam.) The ion current to its collector was maximized and—although the inelastic count rate relative to the background rate was small—some attempt was made to optimize the electron-ion beam overlap by deflecting and focusing only the ion beam to maximize the signal.

Angular distributions in both Zn II and Cd II were measured relative to the intensity at some fixed angle (usually  $14^\circ$ ). Energy-loss spectra at a particular angle were preceded and followed by a spectrum at the  $14^\circ$  (reference) angle to minimize effects of drifts in the ion beam. Recording times were in the range 2–40 min, depending

on the scattering angle, at currents of  $\sim 3 \mu\text{A}$  in both electron and ion beams. Typical spectra of the Cd II  $^2S \rightarrow ^2P$  transitions at 5.472 eV ( $j = \frac{1}{2}$ ) and 5.780 eV ( $j = \frac{3}{2}$ ) are shown in Fig. 2 at 75-eV electron energy. The rising background at energy losses greater than 6.2 eV is due to inelastic electron scattering from the background  $\text{N}_2$  gas, in particular to the  $v' = 0$  onset of the Vegard-Kaplan ( $X^1\Sigma_g^+ \rightarrow A^3\Sigma_u^+$ ) electronic transition. This was noted by recording spectra with the ion-source oven turned off, or by deflecting the ion beam from the scattering center (see below).

Peak areas were measured by drawing a smooth background level beneath the energy-loss feature, and ratios of peak areas or cross sections  $(d\sigma/d\Omega)_\theta / (d\sigma/d\Omega)_{14^\circ}$  were obtained at each scattering angle  $\theta$ . Because of the finite angular resolution of the electron analyzer, and the steeply falling nature of the differential cross section with  $\theta$ , a small correction was applied to this ratio to correct for a "smearing" of the angular distribution. This correction was discussed earlier in reference to work on electron-neutral (He) inelastic scattering.<sup>22</sup> Since the angular acceptance of the present analyzer system was twice that of an earlier system, that correction was double that of earlier work, and amounted to a 2% increase in the Zn II and Cd II data for  $\theta \leq 10^\circ$ , and no correction for data at angles  $10^\circ < \theta \leq 16^\circ$ .

Before discussing conversion of the relative cross sections to the absolute cross-section scale, some consideration should be given to the presence of neutral Cd (and Zn) atoms effusing from the ion-source oven, and to charge exchange of the Cd II (or Zn II) with background

gas to give neutral atoms. Both effects could give rise to spurious inelastic signals simply because the resonance transitions in Cd I and Zn I lie only several tenths of an eV below the resonance lines in the respective ions.<sup>23</sup> To eliminate the possibility of spurious effects several precautions in the original design were taken and diagnostic tests and calculations carried out: First, a straight-through design was *not* employed in the beam line. While a Wien filter was used, a  $3^\circ$  magnetic deflection of the ion beam (see Fig. 1) was inserted, which eliminated neutral species from the ion source by having these strike a baffle at L3 which was itself shielded from the scattering center by the gear wheel. The straight-through path passed 6 cm to one side of the scattering center. A possibility of this effect was tested experimentally in Cd II (and Zn II) by reducing the voltage on a power supply for the electrostatic deflectors in the ion-beam line. A spectrum was first recorded with deflectors "on" (supply at 700 V), then "off" (supply at 100 V). Results of two cycles in this test are shown in Fig. 3. The clear disappearance of the inelastic feature with the supply at 100 V demonstrates that the origin of the feature is ionic since any neutrals from the ion-source oven, unaffected by the electrostatic deflections, would have struck either or both L3 or the gear wheel.

Secondly, while this test appears conclusive, it does not eliminate the possibility that one could have ions present at the entrance to L3, and that these ions could charge exchange with the background gas over the distance  $l$  from L3 to the collision center to again provide neutral Cd I (Zn I) atoms at the collision center. To test this possibility we calculated the fraction  $f$  of the incident ion beam un-

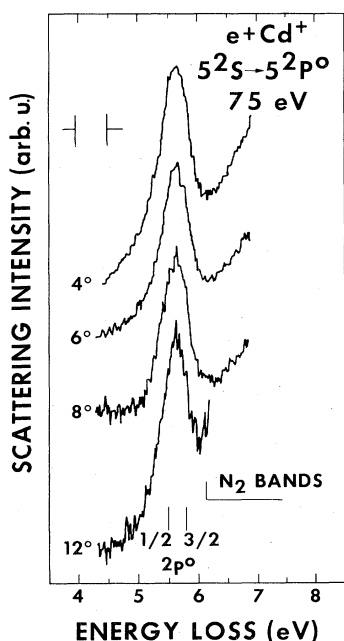


FIG. 2. Energy-loss spectra at the indicated scattering angles for the  $^2S \rightarrow ^2P$  resonance transition in Cd II at an incident electron energy of 75 eV. The overall resolution in the spectra is shown.

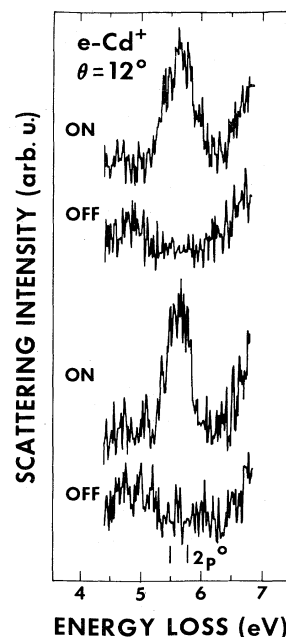


FIG. 3. Diagnostic spectra of the  $^2S \rightarrow ^2P$  transition. Behavior of the feature is shown with deflection voltages at normal settings ("on"), and deflection voltages reduced by a factor of 7 ("off"). Recording time in each case was 3.5 min.

dergoing charge exchange (ce). This is given by  $1 - \exp(-\sigma_{ce}nl)$  where  $\sigma_{ce}$  is the charge-exchange cross section and  $n$  the density of background gas. We could not find in the literature specific cross sections  $\sigma_{ce}$  for 6 keV Cd II or Zn II on  $N_2$  or  $O_2$ . However, one can make liberal estimates of  $\sigma_{ce}$  and  $n$  to get an upper limit to  $f$ . Taking<sup>24</sup>  $\sigma_{ce} \sim 10^{-13}$  cm<sup>2</sup>,  $n \sim 10^9$  cm<sup>-3</sup>, and  $l = 60$  cm one has  $f \sim 6 \times 10^{-3}$ . This is certainly an upper limit. It is also negligible when one considers the additional fact that inelastic scattering cross sections for neutral species are comparable to, or smaller than those for ions.

Finally, we consider the effect of the presence of metastable ions in the beam. In general, barring strong accidental overlaps, metastable ions would not affect the energy-loss spectrum or the relative differential cross sections. However, the final cross section would be affected since metastables would be counted in the ion current  $I_i$ , but not in the inelastic count rate  $\mathcal{R}$ . The flight time from ion source to collision center is 16  $\mu$ sec in the present case, so that lifetimes of metastable states would have to be greater than 4  $\mu$ sec in order to have a 2% or greater effect on the cross section. While lifetimes of highly excited states in Cd II are not known, Shaw *et al.*<sup>25</sup> have measured lifetimes of the  $5^2P_{1/2,3/2}$ ,  $2D_{3/2}$ , and  $2D_{5/2}$  states and obtained values of 3.55, 290, and 720 nsec, respectively. Thus population in at least the low-lying  $2P$  and metastable  $2D$  states would be negligible at the scattering center. The next suitable metastable state is  $4d^95s5p^4P^0$  with levels in the range 13.2–13.9 eV. Accidental overlap would correspond to excitation from these levels into the Cd III ionization continuum (no sharp excitation line).

### III. RESULTS AND DISCUSSION

The inelastic  $2S \rightarrow 2P$  cross section was obtained from a combination of measured and calculated quantities in the equation

$$\frac{d\sigma}{d\Omega} = \frac{\mathcal{R}}{I_i I_e} \frac{e^2 v_i v_e}{(v_i^2 + v_e^2)^{1/2}} \frac{\mathcal{F}}{\Phi \Delta \Omega}, \quad (1)$$

where  $d\sigma/d\Omega$  is the differential cross section (cm<sup>2</sup>/sr),  $\mathcal{R}$  the inelastic scattering count rate (sec<sup>-1</sup>),  $I_i$  and  $I_e$  the ion and electron currents respectively ( $A$ ),  $v_i$  and  $v_e$  the corresponding velocities (cm/sec), and  $e$  the electron charge ( $C$ ). The factor  $\mathcal{F}$  (cm) is the so-called form factor which corrects for spatial inhomogeneities in the densities of both beams. In the case of rectangular-shaped beams it is given by Eq. (7) of Ref. 26 or Eq. (5) of Ref. 14. The quantity  $\Phi \Delta \Omega$  is the product of the transmission-detection efficiency of the electron analyzer ( $\Phi$ ), and the solid angle subtended by the analyzer lens system at the scattering center ( $\Delta \Omega$ ).

The quantities  $\mathcal{R}$ ,  $I_i$ ,  $I_e$ ,  $v_i$ , and  $v_e$  ( $v_e \gg v_i$ ) are all measured or nominally known in the present experiment. In principle the quantities  $\mathcal{F}$ ,  $\Phi$ , and  $\Delta \Omega$  can be measured or at least estimated, and an estimate was given in earlier work on Zn II cross sections based on design parameters and measurements of detection efficiency.<sup>7</sup> For present purposes it was felt more accurate to evaluate the ratio  $\mathcal{F}/\Phi \Delta \Omega$  by calibrating to a calculated cross section<sup>8,27</sup>

for the  $4^2S \rightarrow 4^2P$  transition in Zn II. This was deemed reliable, since (a) the residual electron energies in both the Zn II and Cd II scattering were within several tenths of an eV of one another (75–6.0=69.0 eV in Zn II, 75–5.7=69.3 eV in Cd II), so that effects of variation of  $\Phi \Delta \Omega$  with residual energy in the analyzer system could be neglected, (b) ion and electron focusing procedures were the same in both cases, and (c) the five-state close-coupling calculation was deemed reliable since it gave good agreement with previous integral<sup>14,15</sup> and differential<sup>8</sup> cross-section measurements.

Six determinations of the quantity  $\mathcal{F}/\Phi \Delta \Omega$  in Zn II, on different days and under independent tuning conditions, were made at angles  $\theta$  between 5° and 14°. A value of  $(1.97 \pm 0.37) \times 10^2$  cm was obtained, where the error represents two standard deviations of the mean. This value, when combined with measured quantities in Eq. (1), then gave the differential cross sections at 75 eV. Values of  $d\sigma/d\Omega$  at scattering angles  $\theta$  between 4° and 16° are given in Fig. 4 and Table I. Stated errors represent errors in  $\mathcal{F}/\Phi \Delta \Omega$  and in the measurement of the relative scattering intensities with  $\theta$  combined in quadrature, and are quoted at two standard deviations of the mean. They do not include the systematic uncertainty, believed to be small, of transferring calibration of  $\mathcal{F}/\Phi \Delta \Omega$  from Zn II to Cd II.

For comparison, we have shown in Fig. 4 the calculated differential cross section for the  $4^2S \rightarrow 4^2P$  excitation in Zn II in the same threshold units (80 eV in Zn II versus 75 eV in Cd II). One notes a striking difference in both magnitude and shape of the two cross sections, so that one's expectation that scattering results for these two analogous ions should be comparable is certainly not met.

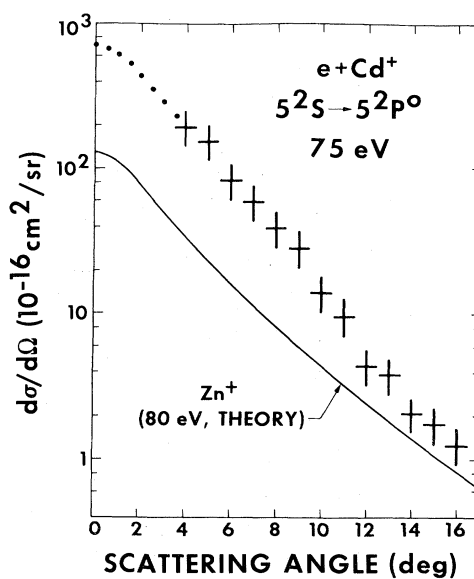


FIG. 4. Experimental differential cross sections in Cd II for the  $5^2S \rightarrow 5^2P$  transition (crosses). Comparison is made with calculated cross sections (Refs. 8 and 27) for the  $4^2S \rightarrow 4^2P$  transition in Zn II at an electron energy (80 eV) corresponding to a comparable fractional energy loss. Dots represent extrapolation to 0° to obtain the integral cross section.

TABLE I. Differential and integral ( $\sigma_I$ ) cross sections for excitation of the  $5^2S \rightarrow 5^2P_{1/2,3/2}$  transition in CdII at 75 eV. Present experimental results are given in column 2, and theoretical results (Refs. 8 and 27) for the  $4^2S \rightarrow 4^2P_{1/2,2/3}$  transition in ZnII at 80 eV in column 3. Entries in parentheses are extrapolated values. Units are  $10^{-16}$  cm<sup>2</sup>/sr.

$\theta$ (deg)	$d\sigma/d\Omega$ (expt.) <sup>a</sup>	$d\sigma/d\Omega$ (theory, 80 eV, Zn II)
0	(735)	128
1	(637)	111
2	(445)	77.5
3	(285)	49.6
4	190±53	33.1
5	152	23.1
6	83.3	16.2
7	58.6	11.6
8	39.0±10.9	8.44
9	28.3	6.07
10	14.0	4.40
11	9.52	3.24
12	4.41±1.23	2.40
13	3.78	1.82
14	2.02	1.42
15	1.73	1.10
16	1.23±0.34	
17	(0.86)	
18	(0.62)	
19	(0.44)	
20	(0.35)	0.284
$\sigma_I(10^{-16}$ cm <sup>2</sup> )	11.3±3.4 <sup>b</sup>	2.48

<sup>a</sup>28% error represents two standard deviations of the mean.

<sup>b</sup>Includes an estimated 3% contribution from  $d\sigma/d\Omega$  at angles  $20^\circ \leq \theta \leq 180^\circ$ . An additional uncertainty reflects the estimated error incurred in extrapolation of  $d\sigma/d\Omega$  from  $4^\circ$  to  $0^\circ$ .

A similarly large cross section was noted by Hane *et al.*<sup>18</sup> in their optical emission measurements of the 214.4-nm line ( $^2P_{3/2} - ^2S_{1/2}$ ) in CdII. One can integrate the present differential results of Fig. 4 and obtain an integral cross section  $\sigma_I$  for the combined  $^2S_{1/2} - ^2P_{1/2,3/2}$  fine-structure components. This integration was carried out by extrapolating  $d\sigma/d\Omega$  from  $\theta=4^\circ$  to  $0^\circ$  using the ZnII (80 eV, theory) differential cross section normalized to the lowest angle,  $\theta=4^\circ$  measurement. Extrapolated values are shown in Fig. 4. Since approximately one-half of  $\sigma_I$  lay in this angular range, several other trial extrapolations were made and the additional systematic uncertainty in  $\sigma_I$  assessed. This error was added linearly to the statistical error in the differential data to give the value of  $\sigma_I$  in Table I.

Results at 75 eV are also shown in Fig. 5 for the sum  $\sigma_I(^2P_{3/2}) + \sigma_I(^2P_{1/2})$ , and for  $\sigma_I(^2P_{3/2})$  alone. The latter quantity was derived from the measured sum by assuming *LS* coupling and a ratio of cross sections of 2:1 for  $\sigma_I(^2P_{3/2}) : \sigma_I(^2P_{1/2})$ ; i.e., just the ratio of statistical weights. The quantity measured by Hane *et al.* (shown in Fig. 5) is an integral cross section for excitation to the  $^2P_{3/2}$  state, but which includes a cascade contribution estimated to be at most 20% of the total.<sup>18</sup> It is gratifying to note that present measurements continue the trend, as

given by the Wigner threshold law and the Bethe theory, of decreasing cross section with increasing electron energy.

While no theoretical calculations were available, we found it interesting to compare our results to semiempirical Gaunt-factor expressions given by Mewe.<sup>19</sup> In this form, the integral cross section can be written as

$$\sigma_I = \frac{8\pi^2 a_0^2}{\sqrt{3}} \left[ \frac{E_H}{E_{ij}} \right]^2 f_{ij} g(U) U^{-1}, \quad (2)$$

where  $a_0$  is the Bohr radius,  $E_H$  the Rydberg energy (13.61 eV),  $E_{ij}$  the transition energy between states  $i$  and  $j$ , and  $f_{ij}$  the corresponding oscillator strength. The quantity  $U$  is the incident electron energy in threshold units ( $U = E_0/E_{ij}$ ), and  $g(U)$  a semiempirical Gaunt factor. For this quantity Mewe has assigned values based on results of experimental measurements and various electron-ion scattering theories. In particular, we compare the CdII  $5s-5p$  transition cross section to an approximate expression for  $g(U)$  suggested by Mewe. This is just

$$g(U) = A + B + C + D \ln U, \quad (3)$$

where the semiempirical constants recommended<sup>19</sup> are  $A=0.6$ ,  $B=C=0$ ,  $D=0.28$  for an allowed transition with no change in principal quantum number.

Calculations of the combined cross section  $\sigma_I(^2P_{3/2}) + \sigma_I(^2P_{1/2})$  were carried out using a weighted transition energy  $\bar{E}_{ij}$  of 5.677 eV and a combined oscillator strength of<sup>28</sup>  $f=0.62$  in Eqs. (2) and (3). Results are shown in Fig. 5. The calculated cross section attains a peak at threshold of  $2.73 \times 10^{-15}$  cm<sup>2</sup> which is a factor of 0.7 the peak value of approximately  $(1 + \frac{1}{2})(2.5 \times 10^{-15}) = 3.75 \times 10^{-15}$  cm<sup>2</sup> from the work of Hane *et al.* At higher energies calculation underestimates the cross section by a factor of 2.5. Both bounds are within the advertised accuracy of the approximation in Eq. (3), but it

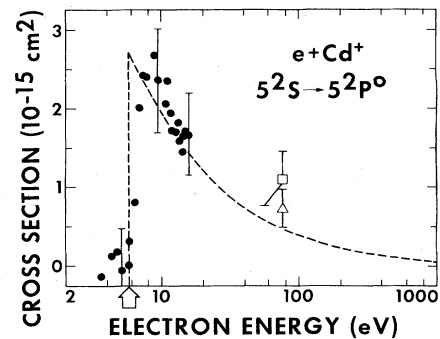


FIG. 5. Integral cross sections for the  $^2S \rightarrow ^2P$  transition in CdII. Filled circles (●) are emission results of Hane *et al.*<sup>18</sup> for the  $^2S_{1/2} \rightarrow ^2P_{3/2}$  fine-structure component, including cascade. Open square (□) is present result for the  $^2P_{3/2}$  and  $^2P_{1/2}$  components, while open triangle (Δ) is present result for the  $^2P_{3/2}$  component alone, assuming *LS* coupling. Dashed line (---) is calculated Gaunt-factor result (Ref. 19) for the  $^2P_{3/2}$  and  $^2P_{1/2}$  components, and gives a peak cross section of  $2.73 \times 10^{-15}$  cm<sup>2</sup> at threshold. The threshold energy is indicated by the vertical arrow.

would be valuable to compare Gaunt-factor calculated results with a more *ab initio* theory in order to assess the form of  $g(U)$  from Eq. (3) for comparison to Cd II.

#### ACKNOWLEDGMENTS

We are very grateful for discussions over several years on various experimental aspects of this work with Dr. K.

T. Dolder, Dr. G. H. Dunn, Dr. M. F. A. Harrison, and Dr. J. Kohl. We thank Dr. A. Z. Msezane and Dr. R. J. W. Henry for results of their Zn II calculations prior to publication. A helpful correspondence with Dr. K. Hane is also acknowledged. This research was carried out at the Jet Propulsion Laboratory, California Institute of Technology, under contract with the U. S. National Aeronautics and Space Administration.

- <sup>1</sup>B. C. Fawcett, *Phys. Scr.* **24**, 663 (1981).  
<sup>2</sup>A. Boksenberg *et al.*, *Nature (London)* **275**, 404 (1978).  
<sup>3</sup>D. E. Shemansky, *Astrophys. J.* **236**, 1043 (1980).  
<sup>4</sup>R. S. Pease, *Contemp. Phys.* **18**, 113 (1977).  
<sup>5</sup>J. L. Cecchi, *J. Nucl. Mater.* **93-94(A)**, 28 (1980); D. E. Post, in *Ion-Ion and Electron-Ion Collisions*, edited by F. Brouliard and J. W. McGowan (Plenum, New York, 1983), p. 37.  
<sup>6</sup>E. Hinnov, *Phys. Rev. A* **14**, 1533 (1976).  
<sup>7</sup>A. Chutjian and W. R. Newell, *Phys. Rev. A* **26**, 2271 (1982).  
<sup>8</sup>A. Chutjian, A. Z. Msezane, and R. J. W. Henry, *Phys. Rev. Lett.* **50**, 1357 (1983).  
<sup>9</sup>D. S. Belić, G. H. Dunn, T. J. Morgan, D. W. Mueller, and C. Timmer, *Phys. Rev. Lett.* **50**, 339 (1983).  
<sup>10</sup>J. B. A. Mitchell, C. T. Ng, J. L. Forand, D. P. Levac, R. E. Mitchell, A. Sen, D. B. Miko, and J. W. McGowan, *Phys. Rev. Lett.* **50**, 335 (1983).  
<sup>11</sup>P. F. Dittner, S. Datz, P. D. Miller, C. D. Moak, P. H. Stelson, C. Bottcher, W. B. Dress, G. D. Alton, N. Nešković, and C. M. Fou, *Phys. Rev. Lett.* **51**, 31 (1983). An estimate of the dielectronic recombination cross section in B III is given by D. J. McLaughlin and Y. Hahn, *Phys. Rev. A* **28**, 493 (1983), and in C IV by the same authors in *Phys. Rev. A* **27**, 1389 (1983).  
<sup>12</sup>See, for example, reviews by K. T. Dolder and B. Peart, *Rep. Prog. Phys.* **39**, 693 (1976); G. H. Dunn, in *The Physics of Ionized Gases*, edited by M. Matić (Boris Kidrić Institute of Nuclear Sciences, Belgrade, 1980), p. 49; D. H. Crandall, *Phys. Scr.* **23**, 153 (1981).  
<sup>13</sup>A preliminary report of this work was given at the XIII International Conference on the Physics of Electronic and Atomic Collisions, Berlin, W. Germany, 1983, abstracts, p. 188; Invited papers (in press).  
<sup>14</sup>W. T. Rogers, G. H. Dunn, J. Østgaard-Olsen, M. Reading, and G. Stefani, *Phys. Rev. A* **25**, 681 (1982).  
<sup>15</sup>A. Z. Msezane and R. J. W. Henry, *Phys. Rev. A* **25**, 692 (1982).  
<sup>16</sup>T. Goto, *J. Phys. D* **15**, 421 (1982).  
<sup>17</sup>K. Hane, T. Goto, and S. Hattori, *J. Phys. D* **15**, L82 (1982).  
<sup>18</sup>K. Hane, T. Goto, and S. Hattori, *Phys. Rev. A* **27**, 124 (1983).  
<sup>19</sup>R. Mewe, *Astron. Astrophys.* **20**, 215 (1972).  
<sup>20</sup>L. Wählin, *Nucl. Instrum. Methods* **27**, 55 (1964); M. Menzinger and L. Wählin, *Rev. Sci. Instrum.* **40**, 102 (1968).  
<sup>21</sup>A. Chutjian, *Rev. Sci. Instrum.* **50**, 347 (1979).  
<sup>22</sup>A. Chutjian, *J. Phys. B* **9**, 1749 (1976).  
<sup>23</sup>From solid-angle considerations alone, a density of  $10^{12}$  atoms/cm<sup>3</sup>, a distance 5 mm from the anode aperture of the ion source, would give a density of  $10^7$  atoms/cm<sup>3</sup> at the scattering center, a distance 160 cm away. This density would then be comparable to the ion density at the scattering center.  
<sup>24</sup>For example, charge-exchange cross sections for ions such as C<sup>+</sup>, N<sup>+</sup>, O<sup>+</sup>, and F<sup>+</sup> on N<sub>2</sub> at an ion velocity of  $\sim 10^7$  cm/s have been reported by various workers to be in the range  $(3-7) \times 10^{-16}$  cm<sup>2</sup>.  
<sup>25</sup>D. A. Shaw, A. Adams, and G. C. King, *J. Phys. B* **8**, 2456 (1975).  
<sup>26</sup>M. F. A. Harrison, *Br. J. Appl. Phys.* **17**, 371 (1966).  
<sup>27</sup>A. Z. Msezane and R. J. W. Henry (private communication); see *Bull. Am. Phys. Soc.* **28**, 798 (1983).  
<sup>28</sup>T. Andersen and G. Sorensen, *J. Quant. Spectrosc. Radiat. Transfer* **13**, 369 (1973).